

**COMPOSITIONAL ANALYSIS OF 21 MARTIAN EQUATORIAL DUNE FIELDS AND POSSIBLE SAND SOURCES.** C. Cornwall<sup>1,2</sup> and T. N. Titus<sup>2</sup>, <sup>1</sup>Northern Arizona University, Flagstaff, AZ 86001 ([cc269@nau.edu](mailto:cc269@nau.edu)), <sup>2</sup>U.S.G.S., 2255 N. Gemini Dr., Flagstaff, AZ 86001 ([ttitus@usgs.gov](mailto:ttitus@usgs.gov))

**Introduction:** There are a total of 547 moderate to large-sized dune fields located within the equatorial region of Mars [1] but only about 60 of those dune fields have adequate data coverage for a study of provenance. Martian dunes are typically isolated and do not have any obvious transport pathways to sand accumulations. Pre-existing pathways may have been erased or wind energy on Mars today may be too weak to sustain transport pathways [2]. It is also possible that sand sources are local and originate from crater or chasma walls. This study focuses on the mineral composition of 21 equatorial dune fields and their surroundings to determine a possible sediment source for each dune field.

**Data:** A total of 21 dune fields were selected among the 547 equatorial dune fields (latitudes between 65°N and 65°S) from the Mars Global Digital Dune Database [1] based on their size (a sinusoidal area greater than ~300) and the amount of Compact Reconnaissance Imaging Spectrometer for Mars (CRISM) coverage. Mineral distributions and relative concentrations inside dune fields as well as outside dune fields were gathered primarily using CRISM data and compared to Thermal Emission Spectrometer (TES) data.

**Analysis:** On average, 50 CRISM footprints were analyzed for each dune field and the surrounding area. CRISM images with small portions of the dune field area were not analyzed to ensure that the spectral index values were from the dune material and not the surrounding area. Footprints outside the dune field included those within a maximum of 850 km radius from the dune field. These footprints also included coverage of the crater wall and floor if the dune field was located inside a crater and that of smaller, neighboring dune fields. Minerals were identified using the indices discussed by Pelkey et al. [3] and the relative concentration of the minerals was determined by threshold values provided by the CRISM team. Hematite index values were treated with caution and compared to TES mineral maps [4], where TES detection of hematite is more reliable. A principle component analysis (PCA) was performed on CRISM index values for each mineral in all 21 dune fields to identify patterns in mineral distributions and concentrations.

**Results:** PCA analysis of the 21 dune field compositions indicates that olivine and monohydrated sulfate minerals have the greatest variance in abundance. Three compositional end members were determined

according to this variance. The first end member corresponded to dune fields poor in olivine and monohydrated sulfates, the second end member consisted of dune fields rich in monohydrated sulfate but poor in olivine, and lastly, the third end member represented dune fields rich in olivine but poor in monohydrated sulfate.

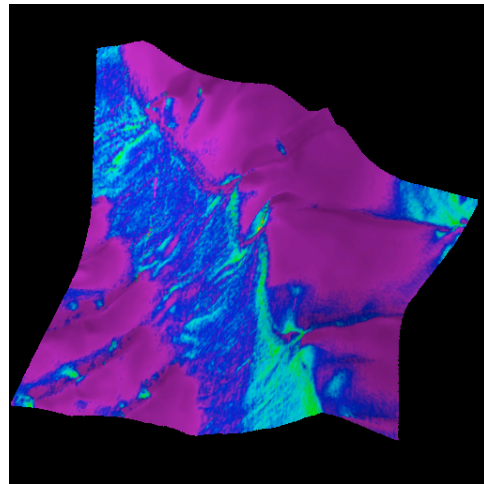


**Figure 1.** CRISM observation FRT 39DF showing the Russell crater mega dune and the presence of olivine on the crest and slope of the dune. Warmer colors indicate a higher olivine concentration.

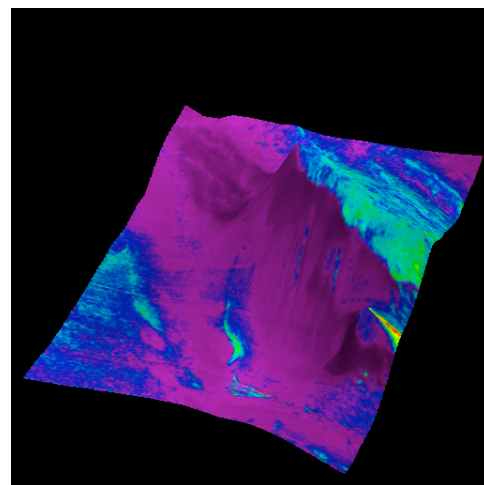


**Figure 2.** CRISM observation FRT 9271 showing the crater wall and floor west of the dune field shown in Figure 1. Warm colors indicate a higher concentration of olivine. The crater floor or rim might be the source of olivine in the dune field 0126-545 (Russell crater).

Many of the dune fields have similar compositions and their differences can be attributed to variations in

mineral concentrations (Table 1). However, a few dune fields had distinct compositions from neighboring dune fields. These dune fields are located in Nili Patera, Juventae and Ganges Chasmata, Meridiani Planum, Proctor crater, Lomonosov crater, and Gale crater. Differences in some of these dune compositions correlate with crater depth. Other compositional differences could be caused by the introduction of wind blown sediments or possible aqueous alterations. In general the composition of dune fields within craters or chasmata were similar to the composition of the walls or floor of the crater or chasma (Fig. 1 and 2).

However, there were four dune fields (Table 1) with a unique composition that did not match the composition of the crater walls or floor, neighboring dune fields, neighboring craters, or the surface mineralogy outside of the craters. These were labeled as “exotic” and presumed to have a distant wind-blown source.

**Summary:** CRISM data and PCA analysis of spectral index threshold values of 21 equatorial dunes indicates that dune sediment compositions have three distinct end members relating to the abundance of olivine and monohydrated sulfate minerals. Further analysis of dune field compositions suggests that the majority of source material is most likely local, coming from the crater or chasma walls but there are a few dune fields that have a potentially distant wind-blown source.

**References:** [1] Hayward et al., (2007), U.S.G.S. Open File Report 2007-1158 [<http://pubs.usgs.gov/of/2007/1158>]. [2] Fenton, L. K. and M. I. Richardson, (2001), *J. Geophys. Res.*, 106(E12) 32,885-32,902. [3] Pelkey et al., (2007), *J. Geophys. Res.*, 112, E08S14, doi: 10.1029/2006JE002831. [4] Bandfield, J. L., (2002), *J. Geophys. Res.*, 107(E6), 5042, doi: 10.1029/2001JE001510.

**Table 1. Summary of minerals present and their relative abundances in the 21 equatorial dune fields from this study. Abundance is based on threshold values for each index. N/A represents lack of data and a single dash signifies the absence of that particular mineral or index inside the dune field. The presence of hematite was often greater in areas of shadow and high albedo. Thus, hematite values shown are typically higher than indicated by TES data. Dune fields labeled as “exotic” are shown in red.**

Dune ID	H2O	Olivine	High Ca Pyrox	Low Ca Pyrox	Sindex	Mono-Hyd Sulf	Fe/Mg	Al	Hematite
2332-530	-	Low	Low	-	Low	-	-	-	-
2404-535	-	-	-	-	Low	Low	Low	Low	Low
2461-581	-	-	-	-	Low	-	-	Low	-
2971-046	-	Low	-	-	Low	Moderate	Low	Low	-
3124-080	-	Low	Low	-	Low	Low	-	Low	-
3352-407	-	Low	Low	-	Low	-	-	Low	-
3403-572	-	-	Low	-	-	Low	Low	Low	Low
3515-596	-	-	-	-	Low	-	-	-	-
3553-642	-	Low	Low	-	-	-	-	Low	-
0126-545	-	Low	Low	-	-	Low	Low	Low	Moderate
0194-468	-	-	Low	-	Low	Low	Low	Low	Moderate
0304-475	-	Low	-	Low	Low	Low	-	Low	Moderate
0347-437	-	-	-	-	Low	Low	-	Low	Low
0045+031	Low	Moderate	Low	-	Low	-	Low	Moderate	-
3513+648	-	-	-	-	-	-	Low	Moderate	-
0443+417	-	Low	Low	-	-	-	-	Low	-
0628+266	-	-	-	-	Low	-	-	Low	-
0671+088	-	Moderate	-	Low	Low	-	Low	Low	-
1249-136	-	Low	Low	-	Low	Low	-	Low	Low
1370-050	-	Low	Low	-	Low	-	-	-	-
1640-615	-	-	-	-	Low	Low	Low	Moderate	N/A